PRECIPITATION AND ARIDITY CONSTRAINTS ON EARLY MARS FROM GLOBALLY-DISTRIBUTED PALEOLAKES. G. Stucky de Quay[1], T. A. Goudge[1], and C. I. Fassett[2], [1]Jackson School of Geosciences, The University of Texas at Austin, Austin, [2]NASA Marshall Space Flight Center, Huntsville, AL. (Contact: g.stucky@utexas.edu)

Introduction: The widespread occurrence of fluvio-lacustrine features on Mars support long-lived flow and accumulation of water in a warmer, wetter past [*1*, *2*]. However, martian climate models have been unable to recreate the necessary conditions required to support a persistent wet climate [*3*–*5*]. Orbital and in-situ datasets have revealed the existence of > 400 paleolakes on Mars, which can be subdivided into open- and closed-basin lakes [*6*–*10*]. Open-basin lakes require that sufficient water accumulated to fill and overtop the basin-confining topography, providing a minimum constraint on required water volumes [*6*–*8*]. Conversely, closed-basin lakes provide maximum water volumes since the absence of an outlet breach generally implies they did not overflow [*6*, *10*]. Importantly, a subset of both open- and closed-basin lakes are fed by valley networks inferred to have been sourced by precipitation during the era of valley network formation > 3.7 Ga [*11*] and may be used to quantitatively constrain precipitation and aridity during early Mars.

Methods: We combine topographic analyses and standard hydrological balances to quantify the time-integrated precipitation for a given lake-breaching wet episode. For each valley network-fed open- and closed-basin lake we compiled three key morphometric measurements: lake area, A_L, lake volume, V_L, and inlet watershed area, A_W (**Fig. 1a,b**). For closed systems, lake dimensions equate to maximum elevation contours before crater rim breaching would have occurred; for open systems, we apply the same method by ignoring the existing outlet to estimate pre-breach geometry. We further classify a subset of lake as *coupled systems*, in which closed- and open-basin lakes are hydrologically connected (**Fig. 1c**). Using a standard water balance equation [e.g. see *8*, *12*] for a given hydrological basin we define a net lake filling rate which is related to measured geometries and evaporation and precipitation rates. Evaporation (i.e. aridity) limits may be constrained from open-basin lake geometries. As such, by integrating the lake filling expression over a given wet episode timescale, τ, we derive minimum and maximum cumulative precipitation, P_τ, for 54 open-basin lakes and 18 closed-basin lakes, respectively.

Results: Precipitation values may be assessed as both a global average or in terms of its spatial variability.

Frequency distribution. Calculated precipitation values are shown in **Fig. 2**. Frequency distributions of

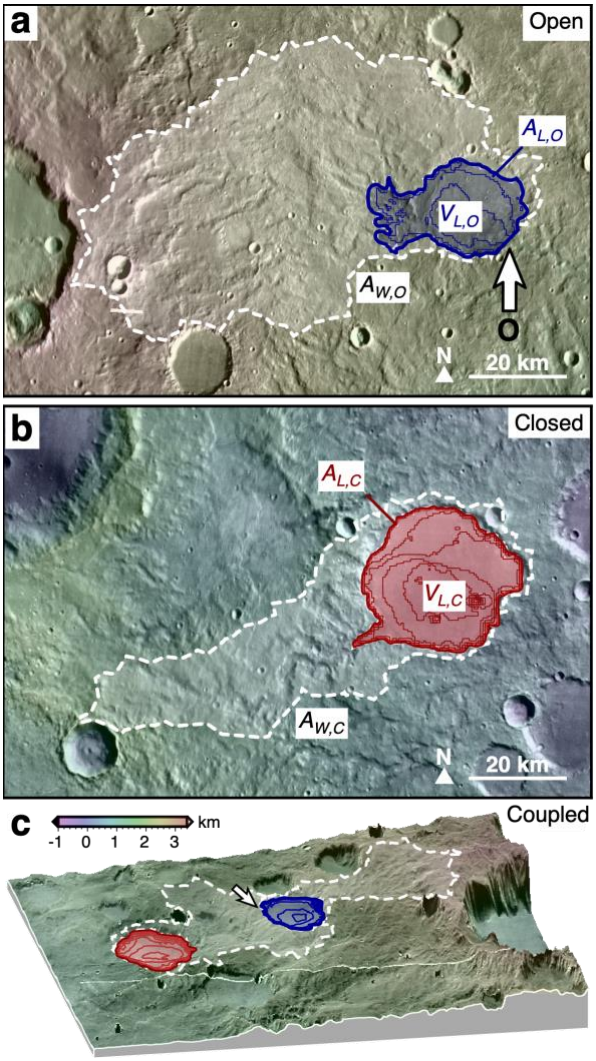

Fig. 1. *Geometries of paleolake basins fed by valley networks on Mars.* ***(a)*** *Open-basin lake; blue polygon = lake area/volume; white dashed line = contributing watershed area; white arrow = outlet canyon (O).* ***(b)*** *Closed-basin lake; red polygon = lake area/volume; white dashed line = contributing watershed area.* ***(c)*** *Coupled system containing both open- and closed- basin lakes. Lake contour lines (= 100 m) and elevation scale bar apply to all three subfigures. Images and elevation data retrieved from THEMIS and MOLA, respectively.*

$P_{\tau,min}$ from open-basin lakes and $P_{\tau,max}$ from closed-basin lakes broadly follow logarithmic normal distributions. The logarithmic means for both open- and closed-basin lake distributions are 4 m and 154 m, respectively. We take these to represent the probable range of minimum and maximum precipitation globally.

Inclusion of groundwater losses or removal of closed-basin lakes with depressed rims do not change these distributions significantly. Coupled systems are represented in **Fig. 2** as individual bounded precipitation values. All are self-consistent such that $P_{\tau,max}$ from the closed-basin lake is always larger than $P_{\tau,min}$ from the connected open-basin lake.

Spatial distribution. Highest minimum precipitations are located around Margaritifer Terra and Terra Sabaea, suggesting these were likely wetter regions. Conversely, lowest maximum precipitations occur in Tyrrhena Terra, suggesting this may have been relatively drier. This is in close agreement with mapped valley network densities that suggest Margaritifer Terra and Terra Sabaea are the most heavily fluvially dissected regions [*1, 13, 14*]. Bounded precipitation values are consistent with a planet-wide wet climate with a complex precipitation pattern, which increases towards the west of Hellas basin. This heterogeneity highlights the importance of incorporating 3-D global climate models to inform the geomorphic evolution of early Mars, which likely cannot be characterized by a single, spatially uniform climate [*3–5, 15*]. The calculated minimum Aridity Indexes, AI, required to breach each open-basin lake suggest the most humid locations on Mars were no more arid than the Great Plains, USA [AI > 0.2; *16, 17*].

Discussion: Current climate models on ancient Mars work towards determining precipitation patterns and the availability of surface water, as well as detangling the relative importance of obliquity, clouds, dust, volcanism, and impacts [*3–5, 18, 19*]. Their relative success and ability to constrain model parameters depends intrinsically on the quantifiability and accuracy of geological predictors. Common challenges with these are that predictors vary over multiple orders of magnitude, are spatially uniform and/or localized, or require climate scenarios that are challenging to recreate. For example, estimated water inventories for early Mars range from ~150 m to > 5000 m GED [global equivalent depth; *20–22*]. Our precipitation limits suggest paleolake basins could have formed with the present-day water inventory ~20 – 30 m GED [*20, 21*]. When combined with previous estimates of martian runoff rates [0.1-60 cm/d; *23, 24*] our precipitation range suggests a wet episode duration of τ ~ 0.2–420 yr with continuous flow (assuming no intermittency). We point out that τ is likely to be only one of many wet episodes in a recurring wet climate, evidenced by the relative amount of incision across the watershed.

Importantly, our morphometric parameters are governed by geometries defined by large-scale topography that is constant over the fluvial timescale and less susceptible to post-fluvial modification. Going forward, our climate optima precipitation and minimum aridity estimates have the potential to work as time-integrated predictors global climate models, improving our fundamental understanding of planetary climate evolution and past habitability of the early martian surface.

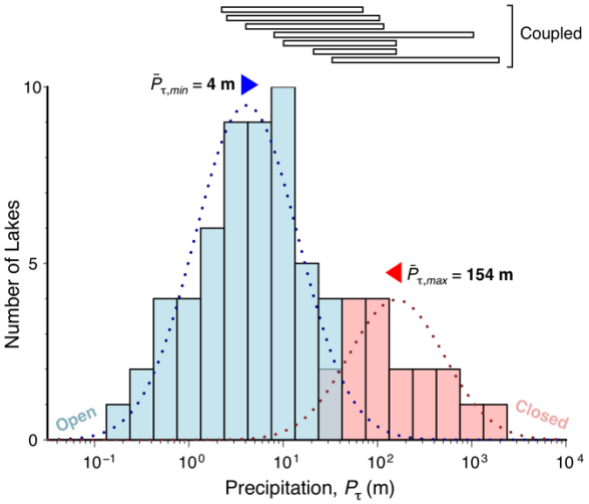

Fig. 2. *Frequency distribution of minimum and maximum precipitation from open- and closed-basin lakes, respectively. Blue/red = open-/closed-basin lakes (n = 54/18); blue/red dotted lines (and triangles) = best-fit logarithmic normal functions for open/closed systems (and logarithmic means); white bars = coupled systems as bounded ranges (n = 7).*

References: [1] Craddock, R. A. & Howard, A. D. (2002) *JGR, 107*. [2] Ramirez, R. M. & Craddock, R. A. (2018) *Nat. Geosci., 11* (2018). [3] Haberle, R. M. (1998) *JGR, 103*. [4] Forget, F., et al. (2013) *Icarus, 222*. [5] Wordsworth, R. D. (2016) *Ann. Rev. of Earth & Plan. Sci., 44*. [6] Cabrol, N. A. & Grin, E. A. (1999) *Icarus, 142*. [7] Cabrol, N. A. & Grin, E. A. (2001) *Icarus, 149*. [8] Fassett, C. I. & Head III, J. W. (2008) *Icarus, 198*. [9] Goudge, T. A., et al. (2012) *Icarus, 219*. [10] Goudge, T. A., et al. (2015) *Icarus, 260*. [11] Goudge, T. A., et al. (2016) *Geology, 44*. [12] Matsubara, Y., et al. (2011) *JGR, 116*. [13] Barnhart, C. J., et al. (2009) *JGR, 114*. [14] Hynek, B. M., et al. (2010) *JGR, 115*. [15] Wordsworth, R., et al. (2013) *Icarus 222*. [16] Trabucco, A. & Zomer, R. (2018) *CGIAR-CSI*. [17] Djebou, D. C. S. (2017) Journ. of Arid Environ. 144. [18] Mischna, M. A., et al. (2003) *JGR, 108*. [19] Palumbo, A. M. & Head, J. W. (2018) *Meteoritics & Planet. Sci., 53*. [20] Carr, M. H. & Head III, J. (2003) *JGR, 108*. [21] Villanueva, G., et al. (2015) *Science*, 348. [22] Luo, W., Cang, X. & Howard, A. D. (2017) *Nat. Comm., 8*. [23] Irwin III, R. P., et al. (2005) *Geology, 33*. [24] Hoke, M. R., et al. (2011) *EPSL, 312*.